THE JOURNAL OF PHYSICAL CHEMISTRY B

Article

pubs.acs.org/JPCB

Heterolytic N–C_α Bond Cleavage in Electron Capture and Transfer Dissociation of Peptide Cations

Matthew D. Wodrich,[†,‡] Konstantin O. Zhurov,[†] Aleksey Vorobyev,[†] Hisham Ben Hamidane,[†] Clémence Corminboeuf,*[,‡] and Yury O. Tsybin*[,†]

[†]Biomolecular Mass Spectrometry Laboratory, Ecole Polytechnique Fédérale de Lausanne, 1015 Lausanne, Switzerland

[‡]Laboratory for Computational Molecular Design, Ecole Polytechnique Fédérale de Lausanne, 1015 Lausanne, Switzerland

Supporting Information

ABSTRACT: Mass spectrometry techniques employing electron capture and electron transfer dissociation represent powerful approaches for the analysis of biological samples. Despite routine employment in analytical fields, the underlying physical processes dictating peptide fragmentation remain less understood. Among the most accepted mechanisms, the Cornell proposal of McLafferty postulates that the homolytic cleavage of N–C_α bonds located in the peptide backbone occurs on the right (C-terminal) side of a hydrogen acceptor carbonyl group. Here, we illustrate that an alternative "enol" mechanism, based on a heterolytic N–C_α bond cleavage located on the left (N-terminal) side of an acceptor carbonyl group, not only is thermodynamically viable but also often represents the energetically preferred cleavage route.

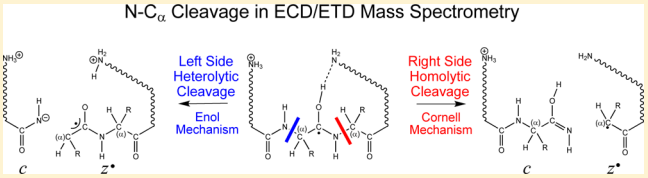

INTRODUCTION

Low-energy electron attachment-mediated fragmentation of multiply charged peptide and protein cations for their structural analysis forms the basis of electron capture and transfer dissociation (ECD and ETD, respectively) tandem mass spectrometry (MS/MS).[1−3] Charge-reduced radical cations are generated in the gas phase through free-electron attachment in ECD[1,2] or electron transfer from a radical anion to multiply charged analyte cations in ETD.[3] These intermediate species dissociate by fast and facile fragmentation of primarily polypeptide backbone N–C_α bonds, producing charged or neutral *c*- and *z*-type products.[2,3] Sequence-specific backbone fragmentation renders ECD/ETD MS/MS a powerful tool for providing peptide and protein primary structure information,[4] characterization of post-translational modifications,[5,6] and insights into protein higher-order structure details.[7,8]

Several mechanisms of N–C_α bond cleavage in ECD/ETD MS/MS have been proposed and studied in detail, both by experimental and by computational means. Among the most prevalent are the "Cornell" mechanism of McLafferty[1] (Scheme 1), the "Washington" and "Utah" mechanisms of Turecek[9] and Simons,[10] respectively, and the "Uppsala" mechanism of Zubarev.[11] In the Cornell mechanism, electron attachment to a local positively charged site is followed by hydrogen atom migration from an N-terminal amine group or a basic amino acid side chain (e.g., lysine, arginine) to a carbonyl oxygen of a proximate amide bond. The aminoketyl intermediate dissociates by homolytic cleavage of the N–C_α bond located on the right side (i.e., in the C-terminal direction) of the carbonyl oxygen, resulting in the formation of *c* and *z* products. The ECD/ETD mechanisms of Turecek and Simons propose that electron capture occurs by a π^* amide orbital, producing a charge-stabilized amide anion-radical intermediate which isomerizes by proton migration to form an aminoketyl radical and, finally, concludes by homolytic N–C_α bond cleavage. The mechanism of Zubarev proposes that electron capture occurs at a neutral hydrogen bond between the backbone nitrogen and carbonyl groups, resulting in production of a negative charge on the nitrogen atom and an aminoketyl radical after an H transfer. The cleavage process then occurs in an identical fashion to that of the Cornell mechanism. Despite their differences, the Cornell mechanism and the mechanisms of Turecek, Simons, and Zubarev each uniquely describe a right-side N–C_α bond rupture. Although no consensus exists on particular mechanistic details, the right-side dissociation pathway is considered the likely cleavage route, as suggested by experimentation[12] and computations on small model peptide systems.[13]

Despite perceived evidence supporting a right-side cleavage mechanism, an alternative pathway in which the ruptured N–C_α bond is located to the left side of the carbonyl group (i.e., toward the N-terminus), has also been considered.[14,15] Possible experimental evidence of this left-side pathway was found in peptide fragmentation studies comparing results from ECD with ETD.[16] However, subsequent studies, in which β-amino acids replaced α-amino acids in order to selectively change the peptide backbone properties, were unable to confirm the existence of the left-side mechanism.[17,18] Computationally, a left-side pathway involving homolytic N–C_α bond cleavage was considered and dismissed for dipeptides.[19] The dismissal of a left-side pathway, in part, may be the result of using small

Received: July 6, 2012
Revised: August 9, 2012
Published: August 13, 2012

Scheme 1. The Cornell ECD/ETD Mechanism in the Tandem Mass Spectrometry of Multiply Charged Polypeptides

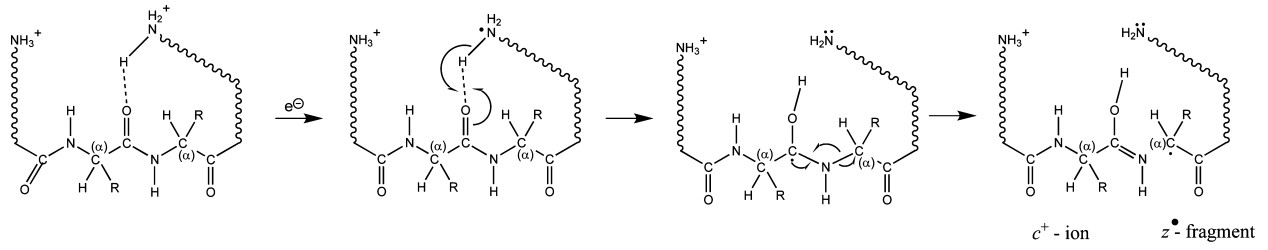

Scheme 2. The Enol ECD/ETD Mechanism in the Tandem Mass Spectrometry of Multiply Charged Polypeptides[a]

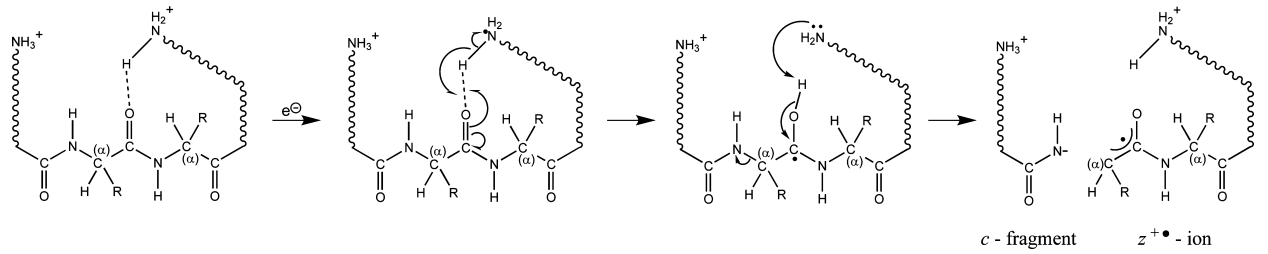

[a]In panel 3, the proton back transfer to the donor amine group may occur either before or after the N–C_α bond cleavage.

organic systems as peptide models, which likely differ from the transition state barrier heights present in real peptide systems. Here, we suggest that a heterolytic left-side cleavage of the N–C_α bond proceeds through an "enol" transition state (Scheme 2) resulting in even-electron *c* fragments and odd-electron *z* ions. The purpose of this work is to show that, contrary to the current paradigm, heterolytic N–C_α bond cleavage in polypeptides through this enol mechanism not only represents a viable alternative to conventional right-side cleavage mechanisms but also in many cases denotes the thermodynamically preferred cleavage route.

METHODS

Computational Details. From a quantum computational perspective, probing the entire conformational landscape of even di- and tripeptides is, generally speaking, beyond current capabilities. While much of the preliminary mechanistic research, including studies addressing ECD/ETD mechanisms, employed small organic systems as peptide surrogates,[9,10,13,20−27] today, systems of increasingly larger size are routinely studied through computation.[15,28−31] Here, 145 conformers of H–Ala_5–Lys–$OH^{+\bullet}$ were used to determine the enthalpies associated with the Cornell and enol N–C_α bond cleavage mechanisms. One hundred forty-five conformers were first constructed ensuring both unique hydrogen bonding patterns and backbone configurations with geometries optimized using MM4.[32] Note that these conformers were chosen to ensure that, upon electron attachment, hydrogen atom migration would occur to each possible carbonyl acceptor group. The set of 145 conformers was examined to guarantee that multiple structures existed where each of the six backbone carbonyl groups acted as a hydrogen atom acceptor. Refined geometries, as radical cations of the 145 conformers, were obtained from optimizations at the B3LYP[33,34]/6-31G(d) level. These radical cation B3LYP geometries were then subject to optimization at the same theoretical level as doubly charged cations (closed shell 2^+) to determine the energetic viability of the parent species. To establish the energetics associated with both the Cornell and enol mechanisms, transition state (TS) geometries were also optimized at the B3LYP/6-31G(d) level and confirmed by examination of their vibrational frequencies (NImag = 1). Since numerous problems are known to exist with respect to the description of the reaction energies of organic compounds using B3LYP,[35] we computed single point energies using both the routinely employed hybrid meta-GGA of Truhlar, M06-2X,[36,37] and a density-dependent dispersion correction to B3LYP (B3LYP-dDsC[38−41]) recently developed by Corminboeuf and co-workers. In its latest comprehensive benchmarking, the dDsC scheme has been shown to dramatically improve the performance of standard functional approximations for various reaction and interaction energies involving peptide conformations, isomerization energies of large molecules, and charge transfer complexes.[42] Broader applications of the approach include the modeling of oxygen reduction reactions by organic reducing agents,[43] the splitting of water by metallocenes,[44] and the description of molecular receptors,[45] all of which involve charged species. The use of such a density-dependent correction is especially pertinent for systems for which density rearrangements (charge transfer and polarization) might influence the reaction energy. Both M06-2X and B3LYP-dDsC single point computations employed a triple-ζ basis set (def2-TZVP). The enthalpies reported throughout include the 298 K ZPE/thermal corrections from B3LYP/6-31G(d) computations appended to M06-2X/def2-TZVP or B3LYP-dDsC/def2-TZVP energies. B3LYP and M06-2X computations employed Gaussian09,[46] while B3LYP-dDsC computations were done using an in-house modified version of Q-Chem.[47]

Experimental Details. The model peptides H–Ala_n–Lys–OH, where n = 3, 4, and 5, were produced by solid phase Fmoc chemistry on an Applied Biosystems 433 A synthesizer, with further purification by liquid chromatography. Peptides were dissolved in water to a concentration of 1 mM and further diluted in a standard electrospray solution (water/acetonitrile 50/50 volume ratio, 0.5% formic acid) to a final peptide concentration of 1 μM. Peptides were ionized using a robotic chip-based nanoelectrospray ionization (ESI) ion source (TriVersa Nanomate, Advion Biosciences, Ithaca, NY) at a

dx.doi.org/10.1021/jp306703f | J. Phys. Chem. B 2012, 116, 10807−10815

flow rate of about 200 nL/min. Mass spectrometric measurements were performed using a hybrid linear ion trap Orbitrap Fourier transform mass spectrometer (LTQ Orbitrap Elite FTMS, Thermo Scientific, Bremen, Germany), equipped with ETD capability[48] and a hybrid linear ion trap 10 T Fourier transform ion cyclotron resonance mass spectrometer (LTQ FT-ICR MS, Thermo Scientific), equipped with ECD capability.[49] The experimental parameters and sequences were controlled by Xcalibur software (Thermo Scientific). Doubly charged precursor ions were isolated in the LTQ with an isolation window of 4 m/z and subjected to either ETD using fluoranthene radical anions (ion−ion interaction time of 100 ms with simultaneous supplemental activation of the charge-reduced species) with reaction products transferred to the Orbitrap FTMS[3] or ECD (low electron energy, electron irradiation period of 70 ms) on the precursor ions first transferred to the ICR FTMS.[1,50] Data analysis was performed with Xcalibur (Thermo Scientific).

RESULTS AND DISCUSSION

The enol mechanism proposed here (Scheme 2) is similar to the Cornell mechanism (Scheme 1) in several ways. Both require explicit hydrogen bonding between a backbone carbonyl oxygen and an N-terminal amine group or a basic amino acid side chain. Electron attachment, presumably to the area of the highest electron affinity,[51] is followed by hydrogen-atom migration from the amine group to the carbonyl oxygen in both mechanisms. The subsequent rearrangement produces an O−H single bond and a $C_{carbonyl}$ centered radical. Here, the two mechanisms diverge. In the Cornell mechanism (Scheme 1), the N−C_α bond is homolytically ruptured, resulting in formation of a C═N bond in the c ion and a radical amide structure in the z product. In the enol mechanism (Scheme 2), heterolytic cleavage results in both electrons from the N−C_α bond being donated to the N atom, producing a local negative charge on the newly formed, zwitterionic c product, whereas the z ion is characterized by a delocalized enol system located on the C_α−$C_{carbonyl}$−O following proton back transfer. The heterolytic nature of the N−C_α bond cleavage is supported by both the iterative Hirshfeld charges,[52−54] which indicate the presence of a significant negative charge on the c-product nitrogen atom (Figure 1) and the spin-density plot, which shows a large amount of spin density over the newly formed enol-like structure of the z product (Figure 2). Also note that in the enol mechanism, c ions may be formed via postfragmentation proton transfer from a z product.

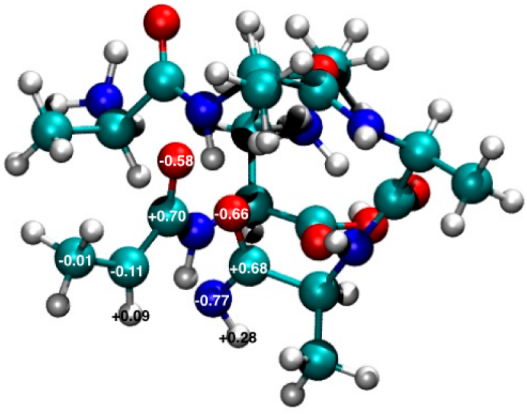

Figure 1. Iterative Hirshfeld charges of selected atoms for a prototypical N−C_α bond cleavage by the enol mechanism at the transition state geometry. Computations are at the B3LYP/6-31G(d) level.

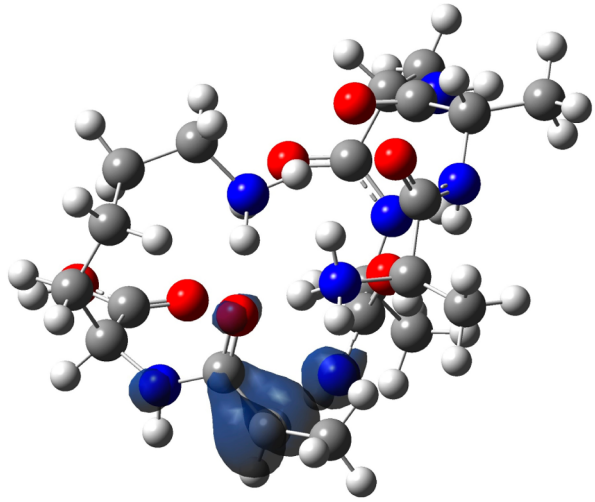

Figure 2. Spin density plot of the enol transition state of a prototypical H−Ala_5−Lys−OH polypeptide. Note the large amount of density delocalized over the C_α−$C_{carbonyl}$ bond in proximity to where the N−C_α bond is broken. This distribution is consistent with a heterolytic N−C_α bond cleavage.

Of the 145 conformers originally constructed, 64 were found to be "low energy" in their open-shell singly charged state (e.g., within 20 kcal/mol of our lowest-energy conformer, Figure 3A), 41 had energies more than 20 kcal/mol above the lowest-energy conformer, and 40 underwent spontaneous NH_3 loss (a commonly observed fragmentation channel in ECD/ETD MS/MS). Note that these energetically low-energy species are likely to be populated, to varying degrees, under standard ECD/ETD MS/MS operating conditions. Of the 64 low-energy conformers, 11 lacked spontaneous hydrogen migration and were not considered further, while 53 had spontaneous hydrogen migration from either the N-terminal or lysine amine group. An examination of the doubly charged parent compounds revealed that the 53 low-energy radical cations arise from a set of 49 distinct parent ion conformers with a range of energies that only slightly exceeds the 20 kcal/mol used to distinguish low-energy radical cations (see the Supporting Information for relative energies of conformers in both their closed-shell doubly charged and open-shell singly charged states).

Of the 53 low-energy radical cation conformers, 20 produced N−C_α bond cleavage through only one mechanism (either Cornell or enol), and 33 conformers, due to the location of the acceptor backbone carbonyl group, have the ability to cleave different N−C_α bonds by a competition between the two mechanisms. Each of these 53 conformers was subjected to cleavage through the Cornell and/or enol mechanisms to determine the most energetically favorable cleavage pathway.

Since the N−C_α bond cleavage considered here occurs only in the proximity of a C═O moiety involved in H bonding with a lysine or N-terminal NH_3^+ group, energetically favorable locations are easily predicted based on the secondary structure of the polypeptide. Cases where hydrogen atom migration is absent (e.g., Scheme 1 and 2 mechanisms terminate before the second step) show greatly increased N−C_α bond cleavage

dx.doi.org/10.1021/jp306703f | J. Phys. Chem. B 2012, 116, 10807−10815

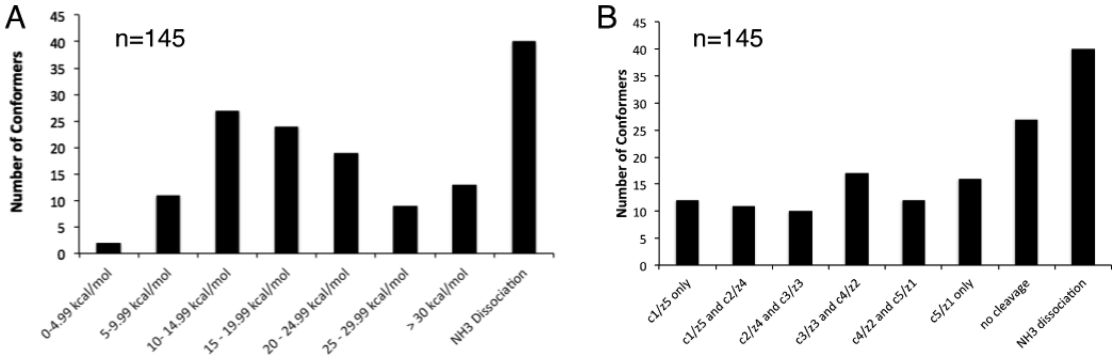

Figure 3. Distribution of the 145 H−Ala$_5$−Lys−OH radical cation conformers by (A) relative energy and (B) anticipated cleavage.

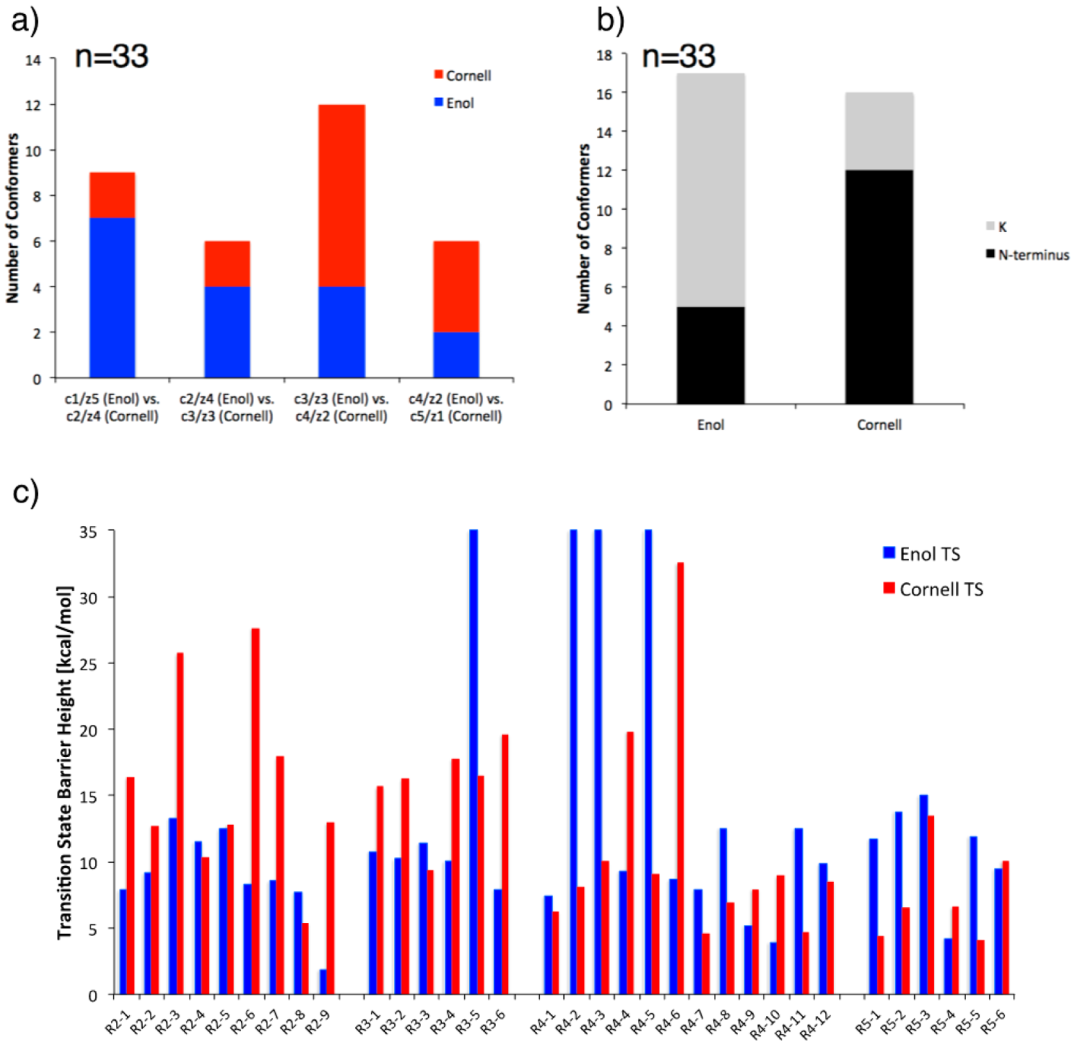

Figure 4. Radical cation H−Ala$_5$−Lys−OH conformer distribution demonstrating (a) the energetically preferred mechanism based on relative cleavage-site location in the peptide backbone, (b) fragmentation mechanism preference as a function of the hydrogen donor (N-terminal or lysine amine group), and (c) the transition state barrier heights from Table 1 for the 33 conformers lying within 20 kcal/mol of the lowest-energy conformer. Note that we were unable to locate enol transition states for the R_3-5, R_4-2, R_4-3, and R_4-5 conformers, which are depicted in (c) as having values of 35 kcal/mol (also see Table 1).

barrier heights (>30 kcal/mol), in contrast to the depressed heights accompanying hydrogen transfer. Each of the bars in Figure 3B corresponds to a set of conformers where the indicated C═O moiety acts as a hydrogen acceptor and the N−C_α bond cleavage leads to production of the indicated c_n and z_m ($n + m = 6$) fragments. The fact that each of these groups contains a minimum of six conformers ensures that any patterns established regarding preferred cleavage mechanism and energy are not based on a single event.

An examination of the energetics involved in the N−C_α bond dissociation process provides several interesting conclusions. The most noteworthy is that the enol mechanism represents

dx.doi.org/10.1021/jp306703f | J. Phys. Chem. B 2012, 116, 10807−10815

Table 1. Relative and TS Enthalpies for H−Ala$_5$−Lys−OH R$_1$−R$_6$ Conformers Along with Predicted Enol and Cornell Products (Computed at the B3LYP-dDsC/def2-TZVP//B3LYP/6-31G(d) and M06-2X/def2-TZVP//B3LYP/6-31G(d) Level), in kilocalories per mole

	relative conformer enthalpy		enol TS			Cornell TS			
species	B3LYP-dDsC	M06-2X	B3LYP-dDsC	M06-2X	enol products	B3LYP-dDsC	M06-2X	Cornell products	donor NH_3 group
R$_1$									
R$_1$-1	0.00	0.00	–	–	–	14.09	18.73	$c_1/z_5^{+\bullet}$	N
R$_1$-2	1.36	1.12	–	–	–	16.81	20.87	$c_1/z_5^{+\bullet}$	N
R$_1$-3	4.04	8.37	–	–	–	14.21	16.88	$c_1/z_5^{+\bullet}$	N
R$_1$-4	8.66	7.59	–	–	–	11.43	16.50	$c_1/z_5^{+\bullet}$	N
R$_1$-5	8.84	10.30	–	–	–	16.83	21.35	$c_1/z_5^{+\bullet}$	N
R$_1$-6	9.06	8.95	–	–	–	3.50	7.90	$c_1/z_5^{+\bullet}$	N
R$_1$-7	9.75	15.28	–	–	–	5.32	9.31	$c_1/z_5^{+\bullet}$	K
R$_1$-8	12.22	14.10	–	–	–	13.36	16.73	$c_1/z_5^{+\bullet}$	N
R$_1$-9	12.82	15.50	–	–	–	5.53	10.26	$c_1^{+}/z_5^{\bullet}$	K
R$_1$-10	14.54	17.33	–	–	–	16.26	20.71	$c_1^{+}/z_5^{\bullet}$	N
R$_2$									
R$_2$-1	5.51	10.19	7.87	11.80	$c_1/z_5^{+\bullet}$	16.41	20.07	$c_2^{+}/z_4^{\bullet}$	K
R$_2$-2	0.99	12.55	9.16	13.63	$c_1/z_5^{+\bullet}$	12.74	18.14	$c_2^{+}/z_4^{\bullet}$	K
R$_2$-3	10.55	14.72	13.30	17.22	$c_1/z_5^{+\bullet}$	25.74	29.66	$c_2^{+}/z_4^{\bullet}$	K
R$_2$-4	10.84	13.34	11.51	14.76	$c_1/z_5^{+\bullet}$	10.40	15.55	$c_2^{+}/z_4^{\bullet}$	K
R$_2$-5	11.89	15.78	12.45	15.00	$c_1^{+}/z_5^{\bullet a}$	12.82	17.07	$c_2^{+}/z_4^{\bullet}$	K
R$_2$-6	13.80	16.59	8.30	11.72	$c_1/z_5^{+\bullet}$	27.67	32.99	$c_2^{+}/z_4^{\bullet}$	K
R$_2$-7	16.19	19.86	8.55	12.09	$c_1/z_5^{+\bullet}$	17.92	21.64	$c_2/z_4^{+\bullet}$	K
R$_2$-8	17.12	19.16	7.69	11.27	$c_1/z_5^{+\bullet}$	5.40	9.81	$c_2^{+\bullet}/z_4$	K
R$_2$-9	18.49	21.32	1.86	4.85	$c_1/z_5^{+\bullet}$	12.96	17.78	$c_2^{+}/z_4^{\bullet}$	K
R$_3$									
R$_3$-1	8.02	11.95	10.78	14.88	$c_2^{+}/z_4^{\bullet a}$	15.67	20.13	$c_3/z_3^{+\bullet}$	N
R$_3$-2	9.15	12.56	10.21	14.02	$c_2^{+}/z_4^{\bullet a}$	16.31	20.71	$c_3/z_3^{+\bullet}$	N
R$_3$-3	12.08	16.71	11.40	14.75	$c_2^{+}/z_4^{\bullet b}$	9.38	14.74	$c_3^{+}/z_3^{\bullet}$	K
R$_3$-4	13.31	15.43	10.03	13.34	$c_2^{+}/z_4^{\bullet b}$	17.79	24.09	$c_3^{+}/z_3^{\bullet}$	K
R$_3$-5	15.48	16.44	–	–	–	16.53	20.67	$c_3/z_3^{+\bullet}$	N
R$_3$-6	17.04	21.56	7.90	10.64	$c_2^{+\bullet}/z_4$	19.63	22.02	$c_3^{+}/z_3^{\bullet}$	K
R$_4$									
R$_4$-1	5.82	7.94	7.40	12.09	$c_3^{+}/z_3^{\bullet}$	6.25	10.79	$c_4/z_2^{+\bullet}$	N
R$_4$-2	7.46	10.43	–	–	–	8.15	11.96	$c_4/z_2^{+\bullet}$	N
R$_4$-3	9.39	11.56	–	–	–	10.04	15.60	$c_4/z_2^{+\bullet}$	N
R$_4$-4	9.42	13.51	9.29	13.63	$c_3/z_3^{+\bullet}$	19.86	22.57	$c_4/z_2^{+\bullet}$	N
R$_4$-5	10.02	13.70	–	–	–	9.10	12.91	$c_4/z_2^{+\bullet}$	N
R$_4$-6	13.78	18.27	8.65	11.25	$c_3/z_3^{+\bullet}$	32.56	38.07	$c_4^{+}/z_2^{\bullet}$	K
R$_4$-7	14.50	17.08	7.92	10.80	$c_3/z_3^{+\bullet}$	4.63	9.53	$c_4/z_2^{+\bullet}$	N
R$_4$-8	15.45	15.77	12.54	20.11	$c_3/z_3^{+\bullet}$	6.97	13.50	$c_4/z_2^{+\bullet}$	N
R$_4$-9	16.22	17.70	5.19	12.08	$c_3/z_3^{+\bullet}$	7.96	13.31	$c_4/z_2^{+\bullet}$	N
R$_4$-10	17.06	22.80	3.93	7.18	$c_3/z_3^{+\bullet}$	8.97	12.15	$c_4^{+}/z_2^{\bullet}$	K
R$_4$-11	18.84	19.36	12.50	17.64	$c_3/z_3^{+\bullet}$	4.68	9.52	$c_4/z_2^{+\bullet}$	N
R$_4$-12	18.85	21.54	9.82	13.57	$c_3/z_3^{+\bullet}$	8.47	11.30	$c_4/z_2^{+\bullet}$	N
R$_5$									
R$_5$-1	7.16	9.40	11.71	9.54	$c_4/z_2^{+\bullet}$	4.44	14.78	$c_5/z_1^{+\bullet}$	N
R$_5$-2	7.78	11.24	13.81	16.62	$c_4^{+}/z_2^{\bullet c}$	6.51	10.91	$c_5/z_1^{+\bullet}$	N
R$_5$-3	13.45	13.79	15.02	18.29	$c_4/z_2^{+\bullet}$	13.48	17.16	$c_5^{+}/z_1^{\bullet}$	K
R$_5$-4	15.79	20.79	4.23	8.15	$c_4/z_2^{+\bullet}$	6.62	11.52	$c_5^{+}/z_1^{\bullet}$	K
R$_5$-5	15.95	19.57	11.92	16.66	$c_4/z_2^{+\bullet}$	4.08	8.20	$c_5/z_1^{+\bullet}$	N
R$_5$-6	16.52	19.60	9.44	15.24	$c_4/z_2^{+\bullet}$	10.08	14.55	$c_5/z_1^{+\bullet}$	N
R$_6$									
R$_6$-1	5.29	8.47	6.39	10.99	$c_5^{+}/z_1^{\bullet d}$	–	–	–	N
R$_6$-2	6.74	7.46	18.86	25.06	$c_5/z_1^{+\bullet}$	–	–	–	N
R$_6$-3	7.01	10.83	4.66	8.63	$c_5^{+}/z_1^{\bullet d}$	–	–	–	N
R$_6$-4	8.26	9.92	2.76	6.74	$c_5^{+}/z_1^{\bullet d}$	–	–	–	K
R$_6$-5	9.65	13.08	9.60	14.09	$c_5/z_1^{+\bullet}$	–	–	–	N
R$_6$-6	11.63	14.21	7.08	12.19	$c_5/z_1^{+\bullet}$	–	–	–	K
R$_6$-7	15.16	16.39	2.05	5.98	$c_5^{+}/z_1^{\bullet d}$	–	–	–	K
R$_6$-8	20.71[e]	27.67	−2.61[e]	−2.54[e]	$c_5/z_1^{+\bullet}$	–	–	–	N

dx.doi.org/10.1021/jp306703f | J. Phys. Chem. B 2012, 116, 10807−10815

Table 1. continued

[a]Proton transfer from the *z* fragment COOH group to the *c* fragment. [b]Proton transfer from a *z* fragment backbone NH to the *c* fragment. [c]Proton transfer from the *z* fragment lysine NH_3 group to the *c* fragment NH cleavage site. [d]Proton transfer from the *z* fragment lysine NH_3 group to the *c* fragment carbonyl oxygen closest to the cleavage point. [e]Relative energy under 20 kcal/mol at the B3LYP/6-31G(d) level. TS energy is 5.23 kcal/mol at the B3LYP/6-31G(d) level.

Scheme 3. Representation of the H−Ala$_5$−Lys−OH Model Peptide[a]

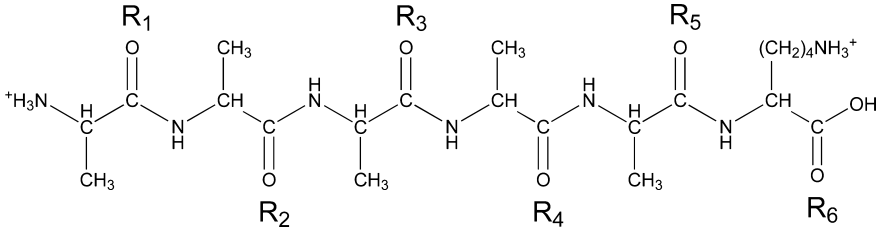

[a]Conformers are labeled by the recipient C═O moiety involved in H transfer upon electron attachment (R_1−R_6). Note that R_2−R_5 conformers may undergo cleavage by either the enol or Cornell mechanisms, whereas the R_1 and R_6 conformers proceed toward fragmentation via a single mechanism only.

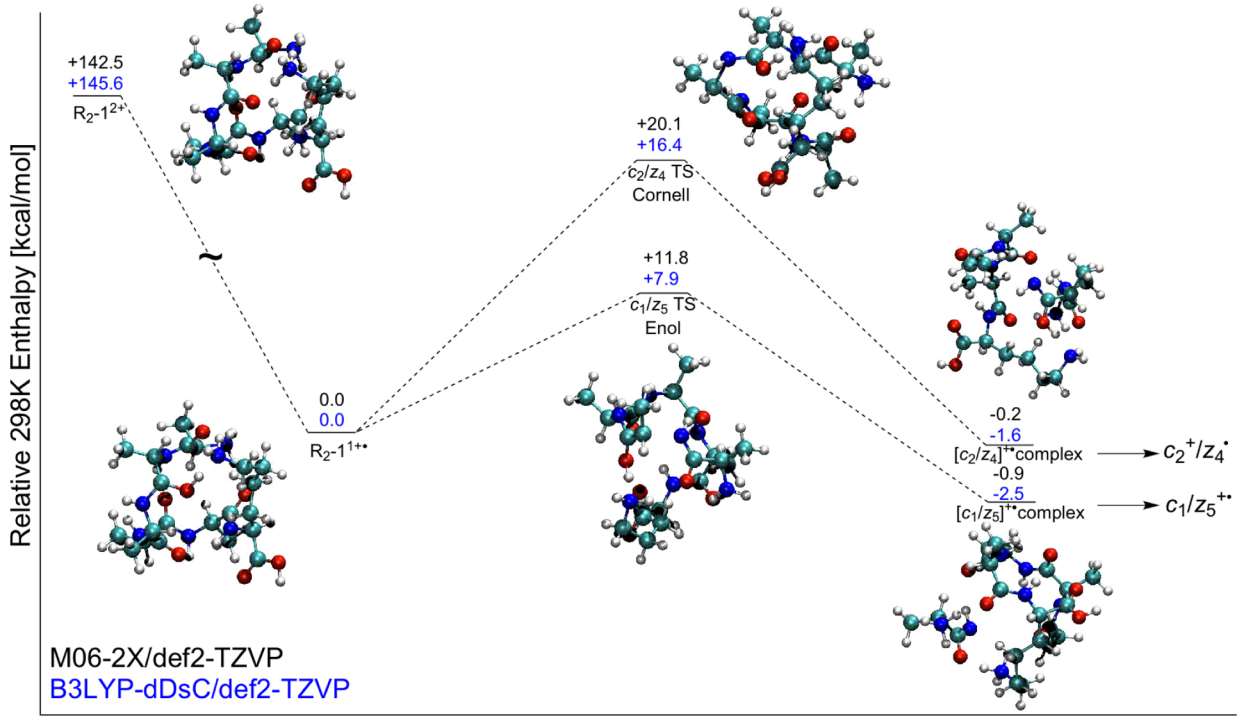

Figure 5. Sample ECD/ETD MS/MS fragmentation pathway for a prototypical H−Ala$_5$−Lys−OH conformer (R_2-1).

the energetically preferred pathway for more than half of the conformers examined (Figure 4 and Table 1). For example, in R_2 conformers (Scheme 3), an energetic competition exists between the enol (products: c_1/z_5) and Cornell (products: c_2/z_4) mechanisms. Naturally, cleavage by each of these mechanisms is associated with a transition state (TS) energy, which must be overcome to form the corresponding products. Our computations reveal that the enol mechanism is energetically preferred over the Cornell mechanism in seven of nine R_2 conformers (Figure 4 and Table 1). The enol mechanism is also favorable for N−C_α bond cleavages of other conformer sets (R_3, R_4, and R_5), although moving away from the N-terminus reduces the frequency of observed cleavages by this mechanism (Figure 4a). A closer examination of the R_2−R_5 conformer structures indicates that the enol mechanism is more energetically favorable when hydrogen atom donation occurs from the lysine NH_3 (Figure 4b), as the larger degree of freedom allows for an increased number of low-energy conformers. Also, note that several instances exist where hydrogen donation from the N-terminal amine group also produces N−C_α bond cleavage through the enol mechanism (e.g., R_3-1, R_4-4, R_5-6, Figure 4c and Table 1). In contrast, R_4 and R_5 conformers tend to accept a hydrogen atom from the N-terminal NH_3, resulting, predominately, in cleavage through the Cornell mechanism. Similar findings were also revealed for smaller polypeptide systems (H−Ala$_4$−Lys−OH, Table S3, and H−Ala$_3$−Lys−OH, Table S4, of the Supporting Information).

Figure 5 represents a prototypical example of the complete reaction processes leading to fragmentation in ECD/ETD MS/MS. Conformers first exist in their doubly charged state, which

dx.doi.org/10.1021/jp306703f | J. Phys. Chem. B 2012, 116, 10807−10815

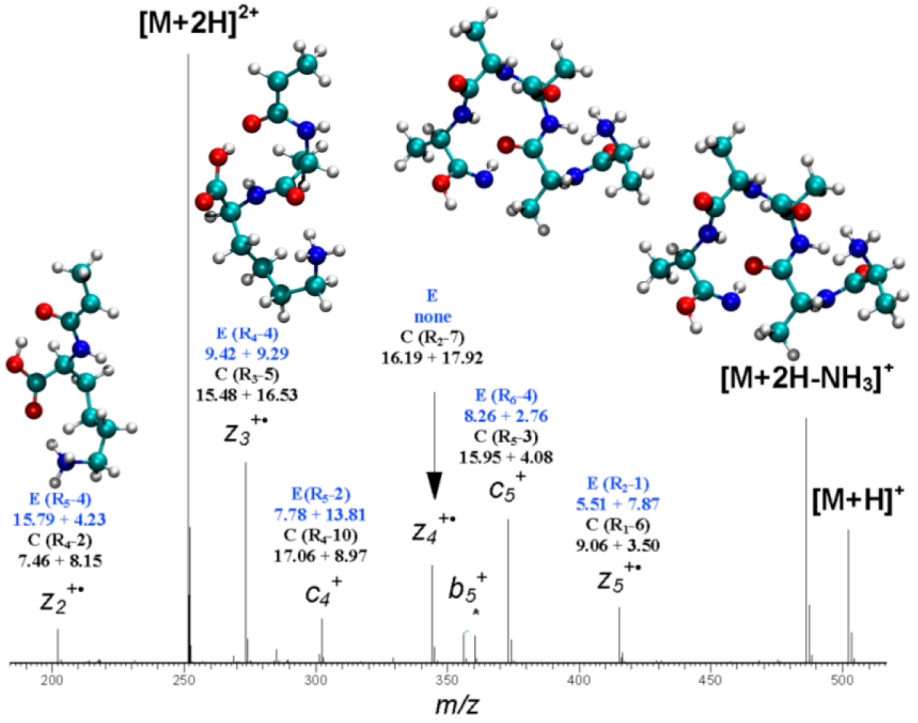

Figure 6. ETD Orbitrap FTMS of doubly protonated H−Ala$_5$−Lys−OH. The assignment above each peak gives both the relative conformer energy (first value, in kilocalories per mole) and the TS barrier (second value, in kilocalories per mole) for both the enol (E, blue) and Cornell (C, black) mechanism.

readily undergoes electron attachment to form the singly charged radical cation. Fragmentation then occurs through N−C$_\alpha$ bond cleavage via the enol or Cornell mechanism, each of which is governed by TS barriers that lead, penultimately, to a $[c + z]^{+\bullet}$ complex and, ultimately, to fully dissociated fragments. As indicated in Figure 5, for the lowest-energy "R$_2$" conformer (R$_2$-1, see Table 1), the lower TS barrier involves dissociation through the enol mechanism, which lies ∼8 kcal/mol below the Cornell pathway at both the M06-2X/def2-TZVP and B3LYP-dDsC/def2-TZVP theoretical levels. The resulting stabilities of the $[c + z]^{+\bullet}$ product complexes are nearly equivalent, indicating that there is no thermodynamic preference for molecule/ion product complexes formed through the conventionally accepted pathways (e.g., Cornell). In fact, the thermodynamic preference for one product set does not necessarily correspond to the TS barrier height governing their formation. In other words, some conformers with lower TS barrier heights have less thermodynamically favorable product complexes. Thus, fragmentation processes preferring to proceed through a Cornell-type cleavage may yield less stable products than those through a higher-energy enol pathway, or vice versa (see the Supporting Information for the full energetics of the "product $[c + z]^{+\bullet}$ complexes").

Note that while we have provided a thermodynamic rationale for the existence of the enol mechanism, accessing kinetic information is more difficult. The kinetics of the reactions until the point of N−C$_\alpha$ bond cleavage should be equivalent, since both the Cornell and enol pathways proceed by identical structures until cleavage occurs. However, dissociation of the final $[c + z]^{+\bullet}$ complex is a necessary step to experimentally observe any product ions. Thus, an additional kinetic issue of interest is how the zwitterionic c fragment dissociates from the $z^{+\bullet}$ in the enol mechanism relative to the $c/z^{+\bullet}$ pair formed in the Cornell mechanism. While we are unable to provide a definitive answer, it is likely that in some cases the enol-formed $[c + z]^{+\bullet}$ complex may have a longer lifetime resulting from attraction between the negative charge on the zwitterionic c fragment and the positively charged amine group of the z ion. On the other hand, a geometric rearrangement of the zwitterionic c fragment after the N−C$_\alpha$ bond cleavage could lead to intrafragmental charge annihilation and to a $[c + z]^{+\bullet}$ complex that dissociates on the same time scale as the product complex formed through the Cornell mechanism. A final possibility is nullification of the zwitterionic c fragment's negative charge by proton transfer from the z fragment. In fact, our computational results support exactly this type of situation (vide infra).

To search for an experimental signature of the N−C$_\alpha$ bond cleavage occurring through the enol mechanism, we performed ECD and ETD MS/MS on isolated doubly protonated H−Ala$_n$−Lys−OH peptides, when n = 3−5 (Figure 6 and Figures S3−S7 of the Supporting Information). Figure 6 shows the ETD mass spectrum of H−Ala$_5$−Lys−OH obtained under standard experimental conditions. To link theory and experiment, we computationally determined specific charge and multiplicity combinations of c and z products formed during the N−C$_\alpha$ bond rupture for each of the 53 low-energy conformers, allowing an association between a specific conformer and an experimental MS/MS peak. As such, each prominent peak in Figure 6 of the ETD mass spectrum shows the specific lowest-energy conformer [along with relative (first value) and TS (second value) energies] leading to its production by both the enol (denoted "E") and Cornell (denoted "C") mechanisms. Since both mechanisms result in the production of identical fragments, direct experimental confirmation of the enol mechanism remains elusive. However, several features of the mass spectra are worth noting. First, for several of the observed peaks ($z_3^{+\bullet}$, c_4^+, and c_5^+), the lowest-

dx.doi.org/10.1021/jp306703f | J. Phys. Chem. B 2012, 116, 10807−10815

energy routes to product ions (the sum of the relative conformer and TS energies) occur through the enol mechanism. If only the TS energies are considered (i.e., that all radical cation conformers are populated to some degree, and only the TS barrier height dictates the rate of production of the observed ions), the number of favored enol routes increases (second values only, Figure 6). Second, although the medium sized $z_4^{+\bullet}$ peak was observed only through a high-energy Cornell pathway for the conformations considered, this same ion could also be produced through a lower-energy enol mechanism (e.g., conformer R_3-1). Our computations reveal that neutral *c* products regularly scavenge a proton from the *z* products, leading to the formation of c^+ ions (see Table 1 for details). This "proton scavenging" behavior is likely indicative of the highly basic character that accompanies the zwitterionic nature of the *c* fragment. However, if the newly formed $[c + z]^{+\bullet}$ complex dissociates rapidly, this proton transfer will not occur, leading instead to $z_4^{+\bullet}$ ions. The relative prominence of this peak may indicate that the fragments produced dissociate in a very rapid manner that precludes back transfer in the final step of the enol mechanism. On the other hand, the presence of the $c_4^{+\bullet}$ suggests a longer-lived $[c + z]^{+\bullet}$ complex,[14,S5,S6] where the *z* product abstracts a hydrogen atom from the *c* ion. Finally, note that differences in the ECD and ETD mass spectra are also apparent (Figures S3−S7 of the Supporting Information). For instance, the ECD mass spectra for each peptide show predominantly *b* and *y* ions, which is explained by an opening of new competitive fragmentation channels brought about by the extra energy imparted by free-electron capture.[S5] Given that the enol mechanism has transition state energy barrier heights similar to those of the Cornell mechanism, these observed differences between ETD and ECD mass spectra remain consistent with both mechanisms.

CONCLUSION

In this article we have suggested that N−C_α bond cleavage may occur through both a right-side Cornell mechanism and a left-side enol mechanism for prototypical peptide systems containing up to six amino acids. Computational results indicate that, for the N−C_α bond cleavage of many conformers, the enol mechanism is energetically preferred over the Cornell mechanism. This is particularly true when the lysine amine group donates the hydrogen atom that begins the cleavage cascade, resulting in the production of heavier *z*-type products (z_4 and z_5). In contrast, the Cornell mechanism is energetically favored for cleavages occurring closer to the C-terminus. Although experimentally no method for distinguishing the enol and Cornell mechanisms could be elucidated for the systems studied here, our results indicate that the enol mechanism should exist in an energetically competitive fashion together with the Cornell mechanism. As such, an explanation for the peaks observed in ECD/ETD mass spectrometry by product ions formed through the Cornell mechanism may also arise from a complementary role played by the enol mechanism. Further computational studies and the search for an experimental verification of the heterolytic N−C_α bond cleavage presented in this work, are currently underway in our laboratory.

ASSOCIATED CONTENT

Supporting Information

ECD and ETD mass spectra of H−Ala_n−Lys−OH (*n* = 3 and 4), electronic energies, enthalpies, and Cartesian coordinates of 2^+, $1^{+\bullet}$, Enol TS, Cornell TS, product complexes, and separated *c*/*z* products (energies only) are provided. Full citations are included for refs 15, 31, and 46−48. This material is available free of charge via the Internet at http://pubs.acs.org.

AUTHOR INFORMATION

Corresponding Author

*Y.O.T.: e-mail, yury.tsybin@epfl.ch. C.C.: e-mail, clemence.corminboeuf@epfl.ch.

Notes

The authors declare no competing financial interest.

ACKNOWLEDGMENTS

Unige A. Laskay, Luca Fornelli, and Stephan N. Steinmann are acknowledged for assistance and helpful discussions. The Swiss National Science Foundation is gratefully acknowledged for financial support (Project 20021-125147/1).

REFERENCES

(1) Zubarev, R. A.; Kelleher, N. L.; McLafferty, F. W. *J. Am. Chem. Soc.* **1998**, *120*, 3265−3266.
(2) Zubarev, R. *Mass Spectrom. Rev.* **2003**, *22*, 57−77.
(3) Syka, J. E. P.; Coon, J. J.; Schroeder, M. J.; Shabanowitz, J.; Hunt, D. F. *Proc. Natl. Acad. Sci. U.S.A.* **2004**, *101*, 9528−9533.
(4) Cooper, H. J.; Hakansson, K.; Marshall, A. G. *Mass Spectrom. Rev.* **2005**, *24*, 201−222.
(5) Stensballe, A.; Jensen, O. N.; Olsen, J. V.; Haselman, K. F.; Zubarev, R. A. *Rapid Commun. Mass Spectrom.* **2000**, *14*, 1793−1800.
(6) Ge, Y.; Lawhorn, B. G.; El Naggar, M.; Strauss, E.; Park, J.-H.; Begley, T. P.; McLafferty, F. W. *J. Am. Chem. Soc.* **2002**, *124*, 672−678.
(7) Cournoyer, J. J.; Pittman, J. L.; Ivleva, V. B.; Fallows, E.; Waskell, L.; Costello, C. E.; O'Connor, P. B. *Protein Sci.* **2005**, *14*, 452−463.
(8) Cournoyer, J. J.; Lin, C.; Bowman, M. J.; O'Connor, P. B. *J. Am. Soc. Mass Spectrom.* **2007**, *18*, 48−56.
(9) Syrstad, E. A.; Turecek, F. *J. Am. Soc. Mass Spectrom.* **2005**, *16*, 208−224.
(10) Sawicka, A.; Skurski, P.; Hudgins, R. R.; Simons, J. *J. Phys. Chem. B* **2003**, *107*, 13505−13511.
(11) Patriksson, A.; Adams, C.; Kjeldsen, F.; Raber, J.; van der Spoel, D.; Zubarev, R. A. *Int. J. Mass Spectrom.* **2006**, *248*, 124−135.
(12) O'Connor, P. B.; Cournoyer, J. J.; Pitteri, S. J.; Chrisman, P. A.; McLuckey, S. A. *J. Am. Soc. Mass Spectrom.* **2006**, *17*, 15−19.
(13) Turecek, F.; Syrstad, E. A. *J. Am. Chem. Soc.* **2003**, *125*, 3353−3369.
(14) Savitski, M. M.; Kjeldsen, F.; Nielsen, M. L.; Zubarev, R. A. *J. Am. Soc. Mass Spectrom.* **2007**, *18*, 113−120.
(15) Turecek, F.; Chung, T. W.; Moss, C. L.; Wyer, J. A.; Ehlerding, A.; Holm, A. I. S.; Zettergren, H.; Brondsted Nielsen, S.; Hvelplund, P.; Chamot-Rooke, J.; et al. *J. Am. Chem. Soc.* **2010**, *132*, 10728−10740 . Full citation given in the Supporting Information.
(16) Ben Hamidane, H.; Chiappe, D.; Hartmer, R.; Vorobyev, A.; Moniatte, M.; Tsybin, Y. O. *J. Am. Soc. Mass Spectrom.* **2009**, *20*, 567−575.
(17) Ben Hamidane, H.; Vorobyev, A.; Larregola, M.; Lukaszuk, A.; Tourwe, D.; Lavielle, S.; Karoyan, P.; Tsybin, Y. O. *Chem.—Eur. J.* **2010**, *16*, 4612−4622.
(18) Sargaeva, N. P.; Lin, C.; O'Connor, P. B. *J. Am. Soc. Mass Spectrom.* **2011**, *22*, 480−491.
(19) Turecek, F. *J. Am. Chem. Soc.* **2003**, *125*, 5954−5963.
(20) Turecek, F.; Polasek, M.; Frank, A.; Sadilek, M. *J. Am. Chem. Soc.* **2000**, *122*, 2361−2370.
(21) Syrstad, E. A.; Turecek, F. *J. Phys. Chem. A* **2001**, *105*, 11144−11155.
(22) Turecek, F.; Syrstad, E. A.; Seymour, J. L.; Chen, X.; Yao, C. *J. Mass Spectrom.* **2003**, *38*, 1093−1104.
(23) Sawicka, A.; Berdys-Kochanska, J.; Skurski, P.; Simons, J. *Int. J. Quantum Chem.* **2005**, *102*, 838−846.

(24) Sobczyk, M.; Skurski, P.; Simons, J. *Adv. Quantum Chem.* **2005**, *48*, 239−251.
(25) Sobczyk, M.; Anusiewicz, I.; Berdys-Kochanska, J.; Sawicka, A.; Skurski, P.; Simons, J. *J. Phys. Chem. A* **2005**, *109*, 250−258.
(26) Anusiewicz, I.; Berdys-Kochanska, J.; Simons, J. *J. Phys. Chem. A* **2005**, *109*, 5801−5813.
(27) Anusiewicz, I.; Berdys-Kochanska, J.; Skurski, P.; Simons, J. *J. Phys. Chem. A* **2006**, *110*, 1261−1266.
(28) Chung, T. W.; Turecek, F. *Int. J. Mass Spectrom.* **2011**, *301*, 55−61.
(29) Moss, C. L.; Chung, T. W.; Wyer, J. A.; Nielsen, S. B.; Hvelplund, P.; Turecek, F. *J. Am. Soc. Mass Spectrom.* **2011**, *22*, 731−751.
(30) Świerszcz, I.; Skurski, P.; Simons, J. *J. Phys. Chem. A* **2012**, *116*, 1828−1837.
(31) Moss, C. L.; Chamot-Rooke, J.; Nicol, E.; Brown, J.; Campuzano, I.; Richardson, K.; Williams, J. P.; Bush, M. F.; Bythell, B.; Paizs, B.; et al. *J. Phys. Chem. B* **2012**, *116*, 3445−3456 . Full citation given in the Supporting Information.
(32) Allinger, N. L.; Chen, K.; Lii, J.-H. *J. Comput. Chem.* **1996**, *17*, 642−668.
(33) Becke, A. D. *J. Chem. Phys.* **1993**, *98*, 5648−5652.
(34) Lee, C.; Yang, W.; Parr, R. G. *Phys. Rev. B* **1988**, *37*, 785−789.
(35) Steinmann, S. N.; Wodrich, M. D.; Corminboeuf, C. *Theor. Chem. Acc.* **2010**, *127*, 429−442 and references cited therein.
(36) Zhao, Y.; Truhlar, D. G. *Theor. Chem. Acc.* **2008**, *120*, 215−241.
(37) Zhao, Y.; Truhlar, D. G. *Acc. Chem. Res.* **2008**, *41*, 157−167.
(38) Steinmann, S. N.; Corminboeuf, C. *J. Chem. Theory Comput.* **2010**, *6*, 1990−2001.
(39) Steinmann, S. N.; Corminboeuf, C. *Chimia* **2011**, *65*, 240−244.
(40) Steinmann, S. N.; Corminboeuf, C. *J. Chem. Phys.* **2011**, *134*, 044117.
(41) Steinmann, S. N.; Corminboeuf, C. *J. Chem. Theory Comput.* **2011**, *7*, 3567−3577.
(42) Steinmann, S. N.; Piemontesi, C.; Delachat, A.; Corminboeuf, C. *J. Chem. Theory Comput.* **2012**, *8*, 1629−1640.
(43) Olaya, A. J.; Ge, P.; Gonthier, J. F.; Pechy, P.; Corminboeuf, C.; Girault, H. H. *J. Am. Chem. Soc.* **2011**, *133*, 12115−12123.
(44) Ge, P.; Todorova, T. K.; Hatay Patir, I.; Olaya, A. J.; Vrubel, H.; Mendez, M.; Hu, X. L.; Corminboeuf, C.; Girault, H. H. *Proc. Natl. Acad. Sci. U.S.A.* **2012**, *109*, 11558−11563.
(45) Rochat, S.; Steinmann, S. N.; Corminboeuf, C.; Severin, K. *Chem. Commun.* **2011**, *47*, 10584−10586.
(46) Frisch, M. J.; Trucks, G. W.; Schlegel, H. B.; Scuseria, G. E.; Robb, M. A.; Cheeseman, J. R.; Scalmani, G.; Barone, V.; Mennucci, B.; Petersson, G. A.; et al. *Gaussian 09*, revision B.01; Gaussian, Inc.: Wallingford, CT, 2010. Full citation given in the Supporting Information.
(47) Shao, Y.; Fusti-Molnar, L.; Jung, Y.; Kussmann, J.; Ochsenfeld, C.; Brown, S. T.; Gilbert, A. T. B.; Slipchenko, L. V.; Levchenko, S. V.; O'Neill, D. P.; et al. *Phys. Chem. Chem. Phys.* **2006**, *8*, 3172−3191 . Full citation given in the Supporting Information.
(48) McAlister, G. C.; Berggren, W. T.; Griep-Raming, J.; Horning, S.; Makarov, A.; Phanstiel, D.; Stafford, G.; Swaney, D. L.; Syka, J. E. P.; Zabrouskov, V.; et al. *J. Proteome Res.* **2008**, *7*, 3127−3136 . Full citation given in the Supporting Information.
(49) Ben Hamidane, H.; Vorobyev, A.; Tsybin, Y. O. *Eur. J. Mass Spectrom.* **2011**, *17*, 321−331.
(50) Tsybin, Y. O.; Quinn, J. P.; Tsybin, O. Y.; Hendrickson, C. L.; Marshall, A. G. *J. Am. Soc. Mass Spectrom.* **2008**, *19*, 762−771.
(51) Gilson, A. I.; van der Rest, G.; Chamot-Rooke, J.; Kurlancheek, W.; Head-Gordon, M.; Jacquemin, D.; Frison, G. *J. Phys. Chem. Lett.* **2011**, *2*, 1426−1431.
(52) Hirshfeld, F. L. *Theor. Chim. Acta* **1977**, *44*, 129−138.
(53) Bultinck, P.; Van Alsenoy, C.; Ayers, P. W.; Carbo-Dorca, R. *J. Chem. Phys.* **2007**, *126*, 144111.
(54) For discussion on the advantage of Hirshfeld charges see: Gonthier, J. F.; Steinmann, S. N.; Wodrich, M. D.; Corminboeuf, C. *Chem. Soc. Rev.* **2012**, *41*, 4671−4687.
(55) Swaney, D. L.; McAlister, G. C.; Wirtala, M.; Schwartz, J. C.; Syka, J. E. P.; Coon, J. J. *Anal. Chem.* **2007**, *79*, 477−485.
(56) Tsybin, Y. O.; He, H.; Emmett, M. R.; Hendrickson, C. L.; Marshall, A. G. *Anal. Chem.* **2007**, *79*, 7596−7602.